Available online at www.sciencedirect.com
ScienceDirect
Chemical Physics Letters 432 (2006) 222–225
CHEMICAL PHYSICS LETTERS
www.elsevier.com/locate/cplett

Fabrication of gold nanorod self-assemblies from rod and sphere mixtures via shape self-selective behavior

Zhi-Chuan Xu [a,b], Cheng-Min Shen [a], Cong-Wen Xiao [a], Tian-Zhong Yang [a], Shu-Tang Chen [a,b], Hu-Lin Li [b], Hong-Jun Gao [a,*]

[a] *Beijing National Laboratory for Condensed Matter Physics, Institute of Physics, Chinese Academy of Science, Beijing 100080, PR China*
[b] *Department of Chemistry, Lanzhou University, Lanzhou 730000, PR China*

Received 6 July 2006; in final form 12 October 2006
Available online 20 October 2006

Abstract

The ordered gold nanorod self-assemblies on silicon wafer were fabricated from rod and sphere mixtures by self-selective behavior. The as-prepared gold nanorod ordered packing structures show a remarkable shape dependence and prefer to pack together separately from spherical particles. This shape induced self-selective behavior was studied via a series of assemblies of nanorods with different aspect ratio. The capillary force interaction between the surfaces of nanoparticles was proposed to explain the nanorods' self-selective behavior.

1. Introduction

The shape-controlled fabrication and self-assembly of very small structures at nano-scales is a technological goal of great practical and fundamental interest because the properties of nanoparticles are greatly size- and shape-dependent. Important progress has been made over the past few years in the preparation of ordered ensembles of metal and semiconductor nanocrystals [1–4]. For examples, the alkanethiol-derivatized gold nanocrystals can organize themselves spontaneously into complex, ordered two-dimensional arrays [5]. The ferromagnetic FePt nanocrystals superlattice assembled by monodisperse FePt nanoparticles shows novel magnetic properties [6]. Most recently, a wet chemical method developed by Jana et al. to synthesize gold [7] and silver [8] nanorods in aqueous solution has attracted great attention since it provides an easy way to obtain the large amount of well controlled nanorods as compared to electrochemical [9] and photochemical [10] methods. The method involves surfactant directed growth of nanorods from spherical seeds [11] and allows people to directly investigate the growth process by the UV–vis spectrum of a gold nanorod solution right after seed addition [12]. Much efforts have been focused on the development of synthetic methodologies [13] and discussion of formation mechanism [14], however, few studies addressed the well organized gold nanorod blocks [15,16] even though these ordered blocks are greatly expected to offer fundamental scientific opportunities for investigating the influence of size and shape with respect to their collective optical and electronic properties. In this letter, we demonstrate for the first time the fabrication of self-assembled gold nanorods on silicon wafer from a mixture of rods and spheres and explain the nanorod self-selective behavior from the view of capillary force interaction. To study the shape selective effect on particles' spontaneous packing behavior, no modification technique, such as three-step growth [7], size selection [7], presence of $AgNO_3$ [8] or HNO_3 [17], was involved in gold nanorod synthesis and thus by-product spherical Au particles with similar diameter were also present.

2. Experimental

Gold nanorods were synthesized by the wet chemical method developed by Jana et al. [7]. For seed preparation,

* Corresponding author.
E-mail address: hjgao@aphy.iphy.ac.cn (H.-J. Gao).

0009-2614/$ - see front matter © 2006 Elsevier B.V. All rights reserved.
doi:10.1016/j.cplett.2006.10.056

a 20 ml aqueous solution containing 2.5×10^{-4} M $HAuCl_4$ and 2.5×10^{-4} M tri-sodium citrate was prepared in a clean flask. Then, 0.5 ml freshly prepared 0.1 M $NaBH_4$ was added into the solution under stirring. The solution color turned to orange immediately and stirring was continued 20 s after adding $NaBH_4$. The as-prepared gold seeds in 4–5 nm were used in 2–8 h after preparation. For nanorod growth, one-step procedure is employed here. Five conical flasks each containing 10 ml growth solution consisting of 2.5×10^{-4} M $HAuCl_4$ and 0.1 M cetyltrimethylammonium bromide (CTAB), were mixed with 0.05 ml 0.1 M freshly prepared ascorbic acid aqueous solution. Ascorbic acid as a mild reducing agent changed growth solution color from brown–yellow to colorless. Next, a series of seed solution in different volume, 0.025, 0.05, 0.1, 0.15, 0.2 ml, were added into five flasks, respectively. After 2–3 h, all the solution were in dark wine red. To remove excess surfactant, the solutions were centrifuged at 9000 rpm for 10 min for several times. The as-prepared sample was diluted in 4 ml distilled water and centrifuged at 9000 rpm for 20 min. The supernatant is removed carefully by a plastic sucker after centrifugation. The precipitate was re-dispersed in ~1 ml distilled water. The 1 ml solution in black color indicated a high concentration. Then, each sample prepared in same way was dropped 0.025 ml on a clean silicon wafer. The silicon wafers with dropped samples and a small beaker of water were placed under a glass plate. The beaker of water provided a water vapor atmosphere to allow the droplets to be dried slowly and form well self-assembled samples. The dried samples were investigated by a field emission type scanning electron microscope (XL30 S-FEG, FEI Corp.) at 10 kV. The UV–vis absorption spectra of samples were recorded by a Cary IE UV–vis spectrometer.

3. Results and discussion

Fig. 1 shows the UV–vis spectra of as-prepared gold nanorod solutions. We controlled the size of nanorods by

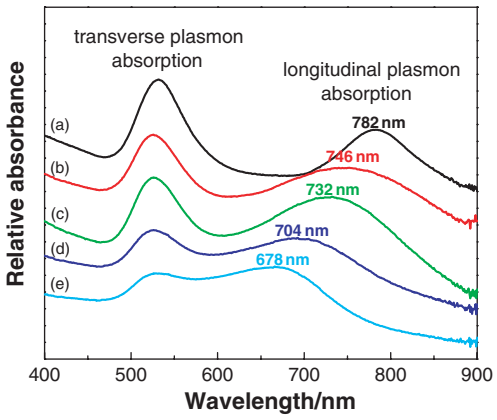

Fig. 1. The UV–vis spectra of as-prepared nanorod solutions: (a) ~18 nm in diameter and ~280 nm in length; (b) ~13 nm in diameter and ~200 nm in length; (c) ~13 nm in diameter and ~140 nm in length; (d) ~13 nm in diameter and ~80 nm in length; (e) ~13 nm in diameter and ~40 nm in length.

varying the volume of seed solution [13]. Without small amount of $AgNO_3$ presence, the yield of rod-like particles is reported before as low as ~30–40% of total particles [18]. The other ~60–70% particles are mostly spherical and their diameter is similar to the rod's transverse size. Similar contribution of rods (~34%) and spheres (~66%) is also found in our experiments. Due to the presence of these spherical particles, the rod transverse absorption band plus the spherical particle surface plasmon absorption band results in stronger transverse plasmon absorption bands than longitudinal ones in the UV–vis spectra. Their longitudinal plasmon bands blue shift from 782 nm to 678 nm indicates a size decrease in rod longitudinal direction, which is confirmed by electron microscope investigations. The rod size for each sample are: (a) ~18 nm in diameter and ~280 nm in length; (b) ~13 nm in diameter and ~200 nm in length; (c) ~13 nm in diameter and ~140 nm in length; (d) ~13 nm in diameter and ~80 nm in length; (e) ~11 nm in diameter and ~40 nm in length.

Fig. 2 shows the typical SEM images of three gold nanorod self-assemblies with different aspect ratios. These self-assembled rods are spontaneously aligned side-by-side and continue this ordered structure in a large scale. For example, some very long 'rod lines' consisting of the side-by-side aligned rods can be observed in longer rod assemblies (Fig. 2a, 2b). Some of these long lines even continue for at least six micron under SEM investigation. The self-assembled nanorods prefer to align side-by-side than end-to-end. In explaining this tendency, one reason is the higher lateral capillary forces along the length of a nanorod as compared to its diameter. It is known that the lateral capillary force for spherical particles is proportional to R^2, in which R is the diameter of particle [19]. And the spontaneous self-assembly of spherical nanoparticles needs a very narrow size distribution (<5%) to take place [20], however, nonspherical nanoparticles show different types of self-assembly. For rod-like particles, two directional capillary interactions at transverse and longitudinal directions should be considered (Fig. 3). Generally, the capillary force (F_{cp}) of small particles for an area projection of A_{xy} with the Laplace pressure Δp is given as

$$F_{cp} = A_{xy}\Delta p \tag{1}$$

the Laplace pressure Δp is defined as

$$\Delta p = (kT \ln p/p_s)/v_0, \tag{2}$$

where k is the Boltzmann constant, T is the system temperature, p/p_s is the relative humidity and v_0 is the molecular volume of the liquid. Eq. (2) implies that Δp is a constant under steady system temperature and humidity. Here, we assume that the nanorods are in perfect rod shape and with smooth hemispherical cross section surface, therefore, the capillary forces at transverse (F_{cpt}) and longitudinal (F_{cpl}) directions can be given as

$$F_{cpt} = A_{xyt}\Delta p, \tag{3}$$

$$F_{cpl} = A_{xyl}\Delta p. \tag{4}$$

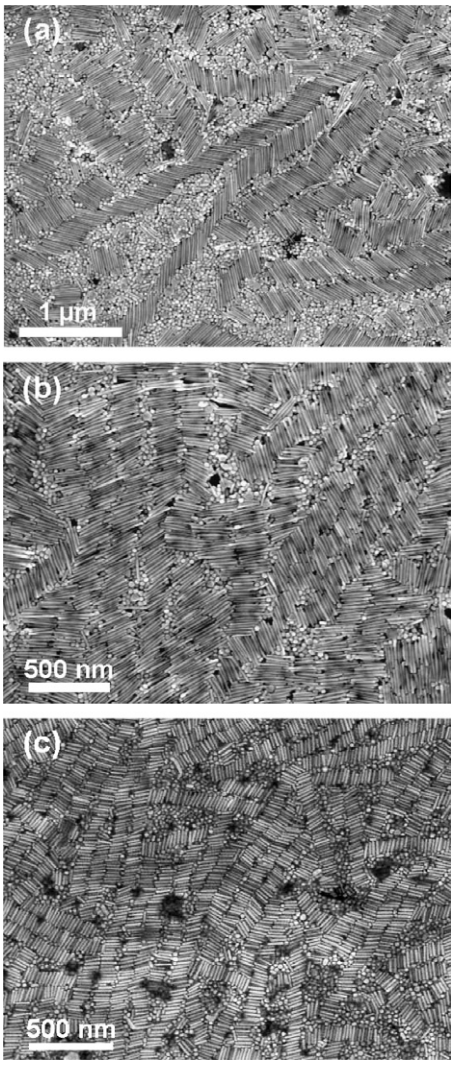

Fig. 2. The typical SEM images of gold nanorod self-assemblies with different aspect ratios and size: (a) ~15.5, (b) ~15.4 and (c) ~6.2.

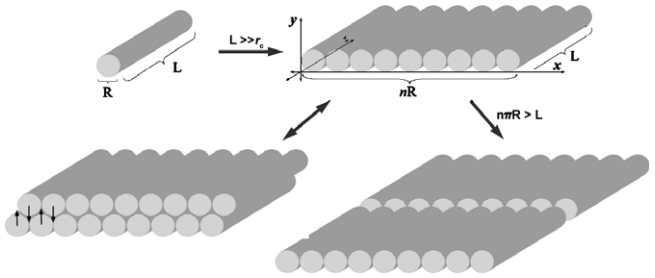

Fig. 3. The possible packing procedure for nanorod self-assembly.

The longitudinal projection area, A_{xyl}, is πr_c^2, where r_c is the radius of the contact line [21]. Similarly, the transverse projection area A_{xyt} can be calculated approximately by $2r_cL$, where L is the rod length. From Eqs. (3) and (4), the capillary force at two directions are:

$$F_{cpl} = \pi r_c^2 \Delta p, \tag{5}$$

$$F_{cpt} = 2r_cL\Delta p. \tag{6}$$

It indicates that the transverse capillary force is always stronger than longitudinal capillary force since $L \gg r_c$ and that makes rod-like particles prefer to align side by side together (Fig. 3).

On the other hand, the rod's transverse capillary force is also stronger much than spherical particle's lateral capillary force. It prevents spheres from intermixing at transverse direction. With the decrease of rod length, the transverse capillary force is weakened. The 'rod lines' such as those observed in longer rod packs show a decrease in their length (Fig. 2c). As shown in Fig. 3, as 'rod ribbons' formed, the directional capillary interactions along y and z axes vertical to 'rod ribbons' are probably produced and work on the 'rod ribbons'. For interaction along y direction, in fact, it is not significant because capillary interaction between nanorods exists along this direction. The superposed 'rod ribbons' will slide into a longer one during solvent evaporation. The other interaction between 'rod ribbons' along z-axis should not be a strong force as well. However, it probably contributes to the phenomena that most 'ribbons' are parallel to each other. This combined capillary force along z-axis (F_{cpz}) can be approximately given as

$$F_{cpz} = A_{xyz}\Delta p \approx 2n\pi R r_c \Delta p, \tag{7}$$

where A_{xyz} is the projection area along z-axis and n is the number of packed nanorods. As long as $n\pi R > L$, the 'ribbons' may have an appealing capillary force interaction along z-axis for parallel assembly.

The anisotropy of interaction between nanorods and that between 'rod ribbons' could be important driving forces for the natural tendency to selectively form ordered structures from a mixture of nanorods and spheres. Thus, the nanorod assembly should not appear everywhere. Fig. 4 shows an optical microscope photograph of a part of sample ring. The sample present on substrate as a ring pattern due to the surface tension and slow evaporation of solvent (water). Corresponding SEM study confirmed that the black region is that where nanorods pack closely together (marked with black arrows) and the others are full filled with spherical particles. In this case, one can differ rods from spheres on a substrate without electron microscope, which may be helpful for further biology application. This spontaneous shape selective packing behavior also could be applied to separate rod-like particles from the mixture of rods and spheres [22].

To determine the stability, the rod self-assembled structures on silicon wafer were maintained at 25 °C and investigated in different time. The self-assembly consisted of rod with diameter ~18 nm, aspect ratio ~15.5 presents a better stability. It could keep its packing structure in nine weeks after preparation (Fig. 5a). The self-assembly of the rod with diameter ~13 nm and aspect ratio ~15.4, however, could not keep their organization as long as the rod with diameter ~18 nm did and they began to lose its ordered structure in five weeks (Fig. 5b) although they both have a similar aspect ratio. The assembly structure of the rod with diameter ~13 nm and aspect ratio ~10.4 began its

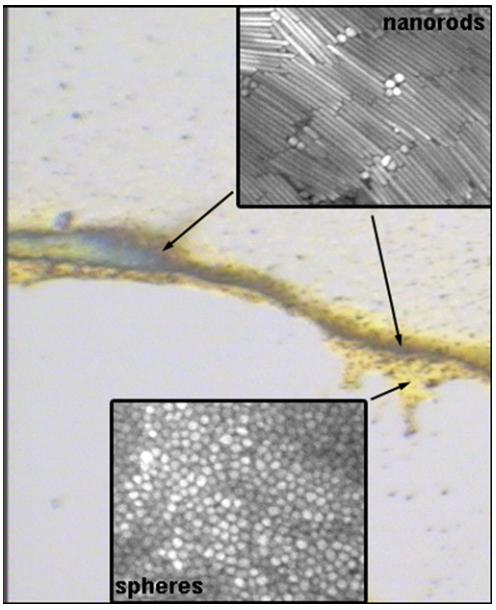

Fig. 4. The optical microscope photograph shows a part of sample ring on silicon wafer. It was revealed by SEM study that the black region is where nanorods pack closely together and yellow region is where spheres present (For interpretation of the references in colour in this figure legend, the reader is referred to the web version of this article).

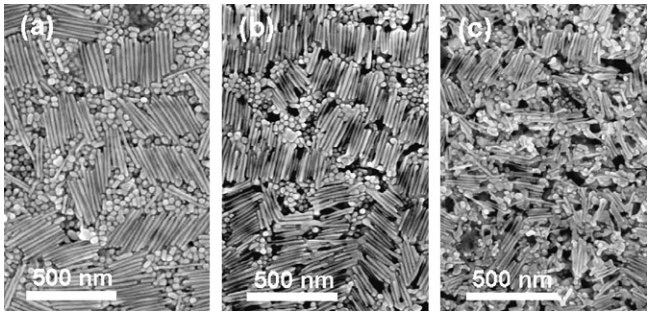

Fig. 5. The SEM images of different rod assemblies observed at different time: (a) the rods with diameter ~18 nm and aspect ratio ~15.5 observed nine weeks after preparation; (b) the rods with diameter ~13 nm and aspect ratio ~15.4 observed five weeks after preparation; (c) the rods with diameter ~13 nm and aspect ratio ~10.4 observed three weeks after preparation.

deformation soon in three weeks (Fig. 5c) and the rod assembly with aspect ratio ~6.2 deformed as quickly as one week. The slight deformation of bigger nanorod assemblies observed in Fig. 5a, 5b probably because the dents and defects inside of particle packing make assemblies subside and deform. Besides inside dents and defects, the serious deformation of smaller rod assembly observed in Fig. 5c is also due to a fact that the rods in small size are instable and show a tendency of shape transformation, which is also found in aqueous solution [23]. Therefore, it can be presumed that the deformation of these rod self-assemblies may be caused by two factors: assembly inside defects and particle shape transformation. Definitely, the stability of the ordered assembly structures is decreased with the rod size decrease.

4. Conclusions

In summary, we have fabricated gold nanorod self-assemblies on the silicon substrate from rod and sphere mixtures via shape self-selective behavior. The self-assembly of gold nanorods shows a remarkable shape dependence and prefers to pack together separately from spherical particles. The capillary force interaction between the surfaces of nanoparticles was proposed to explain the nanorods' self-selective behavior. This behavior may be further applied for biology optical detection and separation. For example, a solution containing two different small bio-molecules can be mixed with Au nanorods and spheres, which are specifically functionalized to bind with the two molecules, respectively. Then the two molecules may be separated on a substrate by this particles' shape self-selective behavior and detected optically at the same time. The detailed study on this now is underway.

Acknowledgements

This work was supported by the National Natural Science Foundation of China (Grant No. 60571045) and National '973' project of China.

References

[1] C.A. Mirkin, R.L. Letsinger, R.C. Mucic, J.J. Storhoff, Nature 382 (1996) 607.
[2] M. Brust, D. Bethell, D.J. Schiffrin, C.J. Kiely, Adv. Mater. 7 (1995) 795.
[3] C.B. Murrary, C.R. Kagan, M.G. Bawendi, Science 270 (1995) 1335.
[4] L. Motte, F. Billoudet, E. Lacaze, J. Douin, M.P. Pileni, J. Phys. Chem. B 101 (1997) 138.
[5] C.J. Kiely, J. Fink, M. Brust, D. Bethell, D.J. Schiffrin, Nature 396 (1998) 444.
[6] S. Sun, C.B. Murray, D. Weller, L. Folks, A. Moser, Science 287 (2000) 1989.
[7] N.R. Jana, L. Gearheart, C.J. Murphy, J. Phys. Chem. B 105 (2001) 4065.
[8] N.R. Jana, L. Gearheart, C.J. Murphy, Chem. Commun. (2001) 617.
[9] Y.Y. Yu, S.S. Chang, C.L. Lee, C.R. Wang, J. Phys. Chem. B 101 (1997) 6661.
[10] K. Esumi, K. Matsuhisa, K. Torigoe, Langmuir 11 (1995) 3285.
[11] J.X. Gao, C.M. Bender, C.J. Murphy, Langmuir 19 (2003) 9065.
[12] B. Nikoobakht, M.A. El-Sayed, Chem. Mater. 15 (2003) 1957.
[13] T.K. Sau, C.J. Murphy, Langmuir 20 (2004) 6414.
[14] C.J. Johnson, E. Dujardin, S.A. Davis, C.J. Murphy, S. Mann, J. Mater. Chem. 12 (2002) 1765.
[15] B. Nikoobakht, Z.L. Wang, M.A. El-Sayed, J. Phys. Chem. B 104 (2000) 8635.
[16] N.R. Jana, Angew. Chem., Int. Ed. 43 (2004) 1536.
[17] H.Y. Wu, H.C. Chu, T.J. Kuo, C.L. Kuo, M.H. Huang, Chem. Mater. 17 (2005) 6447.
[18] N.R. Jana, L. Gearheart, C.J. Murphy, Adv. Mater. 13 (2001) 1389.
[19] P.A. Kralchevsky, K. Nagayama, Langmuir 10 (1994) 23.
[20] C.P. Collier, T. Vossmeyer, J.R. Heath, Annu. Rev. Phys. Chem. 49 (1998) 371.
[21] O.H. Pakarinen et al., Model. Simul. Mater. Sci. 13 (2005) 1175.
[22] N.R. Jana, Chem. Commun. (2003) 1950.
[23] N.R. Jana, L. Gearheart, S.O. Obare, C.J. Murphy, Langmuir 18 (2002) 922.